

Self-consistent random phase approximation in a schematic field theoretical model

T. Bertrand and P. Schuck

CNRS-IN2P3, Université Joseph Fourier, Institut des Sciences Nucléaires, 53, Avenue des Martyrs, F-38026 Grenoble Cedex, France

G. Chanfray

IPN-Lyon, 43 Bd du 11 novembre 1918, F-69622 Villeurbanne Cedex, France

Z. Aouissat

Institut für Kernphysik, Technische Hochschule Darmstadt, Schlossgarten Strasse 9, D-64289 Darmstadt, Germany

J. Dukelsky

Instituto de Estructura de la Materia, C.S.I.C, Madrid, Spain

(Received 19 May 2000; published 5 January 2001)

The exactly solvable model with fermion boson coupling proposed by Schütte and Da Providencia is considered with spontaneously broken symmetry within the so-called self-consistent random phase approximation. Encouraging results for ground and excited states are obtained. A possible extension of the present approach is discussed.

DOI: 10.1103/PhysRevC.63.024301

PACS number(s): 21.60.Jz, 24.10.Cn

I. INTRODUCTION

Application of standard methods of the nonrelativistic many body problem to relativistic field theoretical problems is becoming increasingly popular [1–4]. For instance, the well known random phase approximation (RPA) approach has recently been elaborated in quite some detail [1,2] for field theories of interacting bosons in the linear σ model. This generalizes the well known Gaussian approximation [4], equivalent to a Bogoliubov transformation among the constituents, to the time dependent case. It is, however, well known that standard RPA implies the so called quasiboson approximation [5] violating basic principles of quantum statistics. In general this leads to a quite important overestimation of correlations in the vacuum state [6]. In the past we elaborated an extension of RPA which largely overcomes this deficiency and for which the name self-consistent RPA (SCRPA) was coined. This approach was independently worked out by a second group calling it Cluster-Hartree-Fock (CHF) that seems also very appropriate [7–9]. Improved RPA approaches would also be of great importance for effective chiral Lagrangians and the problem of chiral symmetry restoration. In nuclear physics this approach was introduced a long time ago via the equation of motion method (EMM) by Hara [10] and further elaborated by Rowe [6,11,12]. SCRPA has recently produced quite interesting results in various domains of physics [13–15] and it is our intention here to apply it to a schematic exactly solvable field theoretical model of interacting fermions and bosons first introduced by Da Providencia and Schütte [16]. The application of SCRPA to a boson-fermion model is novel and we will discuss the new features and difficulties which occur.

II. THE MODEL AND SCRPA

The Hamiltonian of the model contains fermions constrained to two levels interacting via a fermion-boson coupling

with

$$H = \bar{n} + ab^+b + G(\tau^+b^+ + \tau^-b) \quad (2.1)$$

$$\begin{aligned} \bar{n} &= \frac{\hat{N}}{2} + \tau^0, \\ n &= \frac{\hat{N}}{2} - \tau^0, \end{aligned} \quad (2.2)$$

where G is the coupling constant, $\hat{N} = n + \bar{n}$ is the particle number operator, and

$$\begin{aligned} \tau^+ &= \sum_k a_{1k}^+ a_{0k}, \quad \tau^- = (\tau^+)^+, \\ \left. \begin{aligned} \hat{N} \\ 2\tau^0 \end{aligned} \right\} &= \sum_{k=1}^{\Omega} (a_{1k}^+ a_{1k} \pm a_{0k}^+ a_{0k}), \end{aligned} \quad (2.3)$$

where τ^+ , τ^- , τ^0 are quasispin operators obeying the usual commutation relation $[\tau^+, \tau^-] = 2\tau^0$, $[\tau^0, \tau^\pm] = \pm\tau^\pm$ and a_{1k}^+ , a_{0k}^+ are fermion creation operators in the upper and lower levels, respectively. The b^+ , b represent a scalar boson. The properties of the model have been well presented in Ref. [16] and we will be very short here.

The Hamiltonian (2.1) describes in a schematic way the field theoretical coupling of fermions to a scalar boson field. The coupling $\tau^+b^+ + \tau^-b$ is such that the transition to a symmetry broken phase of the Nambu-Goldstone type is possible. This is in distinction to other similar models of fermion-boson coupling such as, e.g., the Jaynes-Cummings model [17] where such a phase transition does not show up.

The main feature of the Hamiltonian (2.1) is that it commutes with the symmetry operator

$$P = b^+b - \bar{n}, \quad (2.4)$$

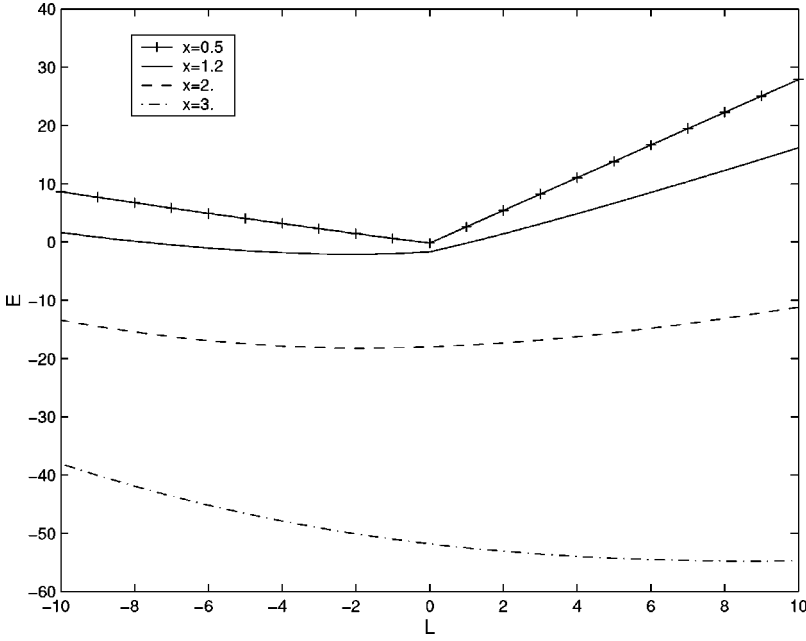


FIG. 1. Ground-state bands for different values of x [see Eq. (2.5)] as a function of L , the eigenvalue of the symmetry operator P of Eq. (2.4).

which accounts for the difference in the number of bosons and the number of fermions in the upper level and that the model possesses, on the mean field level, a continuous spontaneously broken symmetry for

$$x = G \sqrt{\frac{N}{\alpha}} > 1. \quad (2.5)$$

A consequence of the existence of the symmetry operator P with eigenvalue L is that the spectrum of H is grouped into bands (Fig. 1), connecting the lowest states (ground states) for each L value, the first excited states for each L value and so forth. This is depicted in Fig. 1. We see that for $x < 1$ the absolute ground state is always at $L=0$. However, for $x > 1$ the absolute ground state first occurs for $L < 0$, i.e., the system is dominated by a condensate of particle-hole pairs [see Eq. (2.4)] whereas further increase of x shifts the absolute minimum to positive values of L , indicating a condensation of bosons. We henceforth will call the region $x < 1$ the ‘‘spherical’’ region and the region $x > 1$ the ‘‘deformed’’ region.

The Goldstone mode corresponding to the deformed region has been well discussed within the standard RPA in Ref. [16]. For the SCRPA we keep the same RPA operator as proposed in Ref. [16], that is,

$$Q_\nu^+ = X_\nu t^+ - Y_\nu t^- + \lambda_\nu B^+ - \mu_\nu B, \quad \nu = 1, 2, \quad (2.6)$$

where we introduced the following notation:

$$t^\pm = \frac{T^\pm}{\sqrt{-2\langle T^0 \rangle}}. \quad (2.7)$$

The operators T^\pm , T^0 are obtained from τ^\pm , τ^0 in writing the latter ones in the ‘‘deformed’’ basis

$$\begin{pmatrix} \alpha_{1k}^+ \\ \alpha_{0k} \end{pmatrix} = \begin{pmatrix} u & -v \\ v & u \end{pmatrix} \begin{pmatrix} a_{1k}^+ \\ a_{0k} \end{pmatrix}, \quad u^2 + v^2 = 1. \quad (2.8)$$

The boson operators B^+ , B are linked to the original ones by a shift transformation

$$B = b - \sigma, \quad (2.9)$$

where σ is a c -number characterizing the appearance of the Bose condensate. The expectation value $\langle T^0 \rangle$ in Eq. (2.7) is to be evaluated in the RPA vacuum defined through

$$Q_\nu |RPA\rangle = 0. \quad (2.10)$$

The amplitudes in Eq. (2.6) shall obey the following orthogonality relations guaranteeing that the RPA excited state

$$|\nu\rangle = Q_\nu^+ |RPA\rangle \quad (2.11)$$

is normalized, i.e., $\langle \nu | \nu \rangle = 1$:

$$\sum_{\nu=1,2} X_\nu^2 - Y_\nu^2 = 1, \quad \sum_{\nu=1,2} \lambda_\nu^2 - \mu_\nu^2 = 1,$$

$$\sum_{\nu=1,2} \lambda_\nu X_\nu - Y_\nu \mu_\nu = 0, \quad \sum_{\nu=1,2} Y_\nu \lambda_\nu - X_\nu \mu_\nu = 0, \quad (2.12)$$

$$X_\nu^2 + \lambda_\nu^2 - Y_\nu^2 - \mu_\nu^2 = 1, \quad Y_2 X_1 + \mu_2 \lambda_1 - X_2 Y_1 - \lambda_2 \mu_1 = 0,$$

$$X_2 X_1 + \lambda_2 \lambda_1 - Y_1 Y_2 - \mu_2 \mu_1 = 0,$$

with Eq. (2.12), expression (2.6) can be inverted to yield

$$\begin{pmatrix} t^- \\ B \\ t^+ \\ B^+ \end{pmatrix} = \begin{pmatrix} X_1 & X_2 & Y_1 & Y_2 \\ \lambda_1 & \lambda_2 & \mu_1 & \mu_2 \\ Y_1 & Y_2 & X_1 & X_2 \\ \mu_1 & \mu_2 & \lambda_1 & \lambda_2 \end{pmatrix} \begin{pmatrix} Q_1 \\ Q_2 \\ Q_1^+ \\ Q_2^+ \end{pmatrix}. \quad (2.13)$$

The symmetry operator in this ‘‘deformed’’ basis is

$$P = P_0 + P_F + P_B, \quad (2.14)$$

where

$$P_0 = -\frac{N}{2} + \sigma^2,$$

$$P_F = -uv\sqrt{-2\langle T^0 \rangle}(t^- + t^+) + T^0(v^2 - u^2),$$

$$P_B = B^+B + \sigma(B^+ + B).$$

The SCRPA equations are obtained in minimizing the following sum rule (average excitation energy):

$$S_1 = \frac{\sum_{\nu} (E_{\nu} - E_0) |\langle \nu | Q^+ | 0 \rangle|^2 - \sum_{\nu'} (E_0 - E_{\nu'}) |\langle \nu' | Q | 0 \rangle|^2}{\sum_{\nu} |\langle \nu | Q^+ | 0 \rangle|^2 - \sum_{\nu'} |\langle \nu' | Q | 0 \rangle|^2} \quad (2.16)$$

with respect to the RPA amplitudes X , Y , λ , μ [18,19]. In Eq. (2.16) $|\nu\rangle$, $|0\rangle$, E_0 , and E_{ν} are the eigenvectors and eigenvalues corresponding to excited and ground states, respectively. The minimization leads to the following eigenvalue problem:

$$\begin{pmatrix} A_{11} & A_{12} & B_{11} & B_{12} \\ A_{21} & A_{22} & B_{21} & B_{22} \\ -B_{11} & -B_{12} & -A_{11} & -A_{12} \\ -B_{21} & -B_{22} & -A_{21} & -A_{22} \end{pmatrix} \begin{pmatrix} X_{\nu} \\ \lambda_{\nu} \\ Y_{\nu} \\ \mu_{\nu} \end{pmatrix} = \Omega'_{\nu} \begin{pmatrix} X_{\nu} \\ \lambda_{\nu} \\ Y_{\nu} \\ \mu_{\nu} \end{pmatrix}, \quad (2.17)$$

where

$$A_{11} = \langle [t^-, [H', t^+]] \rangle = u^2 - v^2 - 4G\sigma uv \\ + \sqrt{\frac{-2}{\langle T^0 \rangle}} G [u^2(\lambda_1 Y_1 + \lambda_2 Y_2) - v^2(\mu_1 Y_1 + \mu_2 Y_2)],$$

$$A_{12} = \langle [t^-, [H', B^+]] \rangle = -\sqrt{-2\langle T^0 \rangle} G v^2,$$

$$A_{21} = \langle [B, [H', t^+]] \rangle = A_{12},$$

$$A_{22} = \langle [B, [H', B^+]] \rangle = \alpha,$$

$$B_{11} = -\langle [t^-, [H', t^-]] \rangle \\ = \sqrt{\frac{-2}{\langle T^0 \rangle}} G [u^2(X_1 \lambda_1 + X_2 \lambda_2) - v^2(X_1 \mu_1 + X_2 \mu_2)],$$

$$B_{12} = -\langle [t^-, [H', B]] \rangle = G \sqrt{-2\langle T^0 \rangle} u^2,$$

$$B_{21} = B_{12},$$

$$B_{22} = -\langle [B, [H', B]] \rangle = 0. \quad (2.18)$$

In Eq. (2.18) we introduced the cranked Hamiltonian $H' = H - \mu P$ in order to fix the value $L = \langle P \rangle$ in the symmetry broken phase. In the spherical case this extra term is absent.

To obtain expression (2.18) we have made use of Eqs. (2.13), (2.10). For a completely self-consistent solution we still have to establish equations which determine the mean field parameters u , v , and σ and give an expression for $\langle T_0 \rangle$.

The mean field amplitudes are as usual obtained from a minimization of the ground-state energy [5,20]

$$\frac{\partial \langle H' \rangle}{\partial u} + \frac{\partial \langle H' \rangle}{\partial v} \frac{\partial v}{\partial u} = \langle [H', t^+] \rangle = 0, \quad (2.19)$$

$$\frac{\partial \langle H' \rangle}{\partial \sigma} = \langle [H', B^+] \rangle = 0$$

with

$$\langle H' \rangle = (1 + \mu) \left(\frac{N}{2} + (u^2 - v^2) \langle T^0 \rangle \right) + (\alpha - \mu) (\langle B^+ B \rangle + \sigma^2) \\ + G \sqrt{-2\langle T^0 \rangle} \left\{ -4uv \frac{\langle T^0 \rangle}{\sqrt{-2\langle T^0 \rangle}} \sigma + u^2 (\langle t^+ B^+ \rangle \right. \\ \left. + \langle t^- B \rangle) - v^2 (\langle t^- B^+ \rangle + \langle t^+ B \rangle) \right\}. \quad (2.20)$$

Explicitly these equations yield for u , v , and σ

$$-4G\sigma \langle T^0 \rangle v + \mathcal{I}u + (-4G\sigma \langle T^0 \rangle u + \mathcal{K}v) \left(\frac{u}{v} \right) = 0, \quad (2.21)$$

$$u^2 = \frac{1}{2} \left(1 + \frac{\epsilon}{\sqrt{\epsilon^2 + \Delta^2}} \right), \quad v^2 = \frac{1}{2} \left(1 - \frac{\epsilon}{\sqrt{\epsilon^2 + \Delta^2}} \right), \quad (2.22)$$

$$\Delta = 4G \langle T^0 \rangle \sigma, \quad (2.23)$$

$$\epsilon = \frac{\mathcal{K} - \mathcal{I}}{2},$$

with

$$\mathcal{I} = 2[\langle T^0 \rangle + G(Y_1 \lambda_1 + X_1 \mu_1 + Y_2 \lambda_2 + X_2 \mu_2) \sqrt{-2\langle T^0 \rangle} \\ + \mu \langle T^0 \rangle],$$

$$\mathcal{K} = -2[\langle T^0 \rangle + G(X_1\lambda_1 + Y_1\mu_1 + X_2\lambda_2 + Y_2\mu_2)\sqrt{-2\langle T^0 \rangle} + \mu\langle T^0 \rangle]. \quad (2.24)$$

The only unknown at this point which prevents a fully self-consistent solution of the SCRPA equations (2.17) is the expectation value $\langle T^0 \rangle$. As in previous studies for other models [20,21] this quantity poses some problems and its evaluation in terms of the RPA amplitudes is only possible for a ground state explicitly determined using the vacuum condition (2.10). Since we have not achieved to construct |RPA> (this always turns out to be extremely difficult but for very trivial cases), we apply the usual well tested approximation techniques for the evaluation of $\langle T^0 \rangle$. One of the most popular methods consists in inserting the number operators into $\langle T^0 \rangle$ [12]. This method was further developed by Catara [22] and amounts to approximately replacing T^0 by

$$T^0 \equiv -\frac{N}{2} + T^+ T^-. \quad (2.25)$$

A more general expression where T^0 is expanded into a power series in $(T^+)^n(T^-)^n$ is given in Refs. [23–25]. Taking the expectation value and using Eq. (2.13) one arrives at the following expression:

$$\langle T^0 \rangle = \frac{-N/2}{1 + (2/N)(Y_1^2 + Y_2^2)}. \quad (2.26)$$

With Eq. (2.26) the SCRPA equations are now completely closed and we can proceed to the numerical solution.

The direct iterative solution as an eigenvalue problem causes some problems, since in the symmetry broken phase one of the two eigenvalues will appear at very low energy. In the pure RPA limit [Y and μ amplitudes equal zero in RPA matrix (2.17)] this eigenvalue corresponds to the spurious or Goldstone mode at zero energy. However, in the SCRPA as well as in the exact solution this mode comes at a finite, be it at a very small energy. This small eigenvalue in the SCRPA is produced from a square root of a difference of rather large numbers. Any imbalance in the iteration cycle leads to imaginary eigenvalues and to a breakdown of the iteration. We solve this problem in inserting into Eq. (2.17) the explicit form of the eigenvalues

$$\Omega'_\nu = \sqrt{\frac{-\beta \pm \sqrt{\beta^2 - 4\gamma}}{2}}, \quad \nu = 1, 2, \quad (2.27)$$

where

$$\begin{aligned} \beta &= 2(B_{12}^2 - A_{12}^2) - (A_{11}^2 + A_{22}^2 - B_{11}^2), \\ \gamma &= (A_{12}^2 - A_{11}A_{22})^2 - (B_{11}A_{22} - A_{12}B_{12})^2 + (B_{12}^2 - A_{11}A_{22})^2 \\ &\quad - A_{12}^2 B_{12}^2 - A_{11}^2 A_{22}^2 + 2A_{12}A_{22}B_{11}B_{12}. \end{aligned} \quad (2.28)$$

This gives eight homogeneous nonlinear equations for the eight unknowns X_ν , Y_ν , λ_ν , μ_ν . These equations are solved together with the two constraints of normalization

$$X_\nu^2 + \lambda_\nu^2 - Y_\nu^2 - \mu_\nu^2 = 1, \quad \nu = 1, 2 \quad (2.29)$$

as a set of nonlinear equations for the amplitudes.

Naturally this is done with a simultaneous solution of the mean-field equations (2.19), (2.21) and in the symmetry broken phase under the further constraint that the value of μ gives exactly

$$\langle P \rangle = L \quad (2.30)$$

which corresponds to the quantum number of the symmetry operator we have chosen to consider. We also can calculate the RPA eigenvalue Ω' which, as the ground-state energy, should be corrected for the contribution of the constraint [13]

$$\Omega_\nu = \Omega'_\nu + \mu \langle [Q_\nu, [P, Q_\nu^+]] \rangle. \quad (2.31)$$

The explicit expression in terms of the RPA amplitudes reads

$$\Omega_\nu = \Omega'_\nu + \mu[(v^2 - u^2)(X_\nu^2 + Y_\nu^2) + \lambda_\nu^2 + \mu_\nu^2]. \quad (2.32)$$

III. RESULTS

We now come to the presentation and the discussion of the results. In the first place we want to mention that the model turned out to be somewhat unfortunate, since for several quantities the differences between standard RPA and SCRPA are very small as well as their respective differences with the exact solution. This feature is relatively independent of the parameters of the model. Nonetheless SCRPA shows always a clear superiority over standard RPA and we also can isolate some quantities where SCRPA presents strong improvement. Let us start with the ground-state energy. In Table I we show the absolute ground-state minima for $\alpha = 3$, $N = 30$ as a function of x [Eq. (2.5)] for the exact case and for RPA and SCRPA. As we have seen in Sec. II the lowest eigenvalue of H for different values of x in the “deformed” region belongs to different values of L . We therefore give in Table I also the corresponding L values as well as the values of the Lagrange multiplier μ .

From Table I we see the following. In the nondeformed region the SCRPA performs extremely well for the ground state up to the phase transition point $x = 1$. The differences with the exact ground state are only in the fourth significant digit. A very satisfying feature also is that, contrary to standard RPA, the SCRPA energies consistently are *above* the exact energies. Indeed it is so far an unproven conjecture that SCRPA yields an upper bound to the exact ground state. Shortly after the phase transition $x \approx 1$ the situation deteriorates somewhat but qualitatively it stays the same: standard RPA overbinds and SCRPA underbinds. However, as x increases both E_{RPA} and E_{SCRPA} move up with respect to the exact value E_0 . Between $x = 1.4$ and $x = 1.5$ also E_{RPA} crosses from over binding to under binding. There is a situation where artificially E_{RPA} becomes equal to the exact value, whereas E_{SCRPA} lies above the exact value at the same x value. All this reflects the well-known fact that standard RPA over estimates the correlations due to the violation of the Pauli principle. Due to this feature, for values of $x > 1.5$, E_{RPA} stays artificially closer to the exact value than

TABLE I. Exact (E_0), RPA, and SCRPA energies, L values, and the ‘‘chemical potential,’’ μ , calculated with SCRPA, for the spherical and deformed regions.

x	L	μ	E_0	E_{RPA}	E_{SCRPA}
0.1	0		-0.007513	-0.007514	-0.007513
0.2	0		-0.030213	-0.030228	-0.030212
0.3	0		-0.068597	-0.068679	-0.068596
0.4	0		-0.123554	-0.1238	-0.123554
0.5	0		-0.196474	-0.197224	-0.196472
0.6	0		-0.289436	-0.2912	-0.289429
0.7	0		-0.405551	-0.4094	-0.405531
0.8	0		-0.5496	-0.55777	-0.54954
0.9	0		-0.729369	-0.747	-0.72914
1.0	0		-0.958	-1	-0.9576
1.1	-1	-0.049	-1.326	-1.378	-1.296
1.2	-2	-0.009	-2.112	-2.15	-2.041
1.3	-3	-0.044	-3.256	-3.277	-3.154
1.4	-3	0.032	-4.715	-4.720	-4.591
1.5	-3	0.063	-6.425	-6.417	-6.284
1.6	-3	0.055	-8.380	-8.364	-8.227
1.7	-3	0.018	-10.555	-10.535	-10.395
1.8	-3	-0.037	-12.921	-12.899	-12.755
1.9	-2	0.04	-15.475	-15.449	-15.308
2.0	-2	-0.044	-18.218	-18.192	-18.05
2.1	-1	-0.003	-21.137	-21.112	-20.97
2.2	0	0.022	-24.219	-24.194	-24.055
2.3	1	0.034	-27.468	-27.445	-27.31
2.4	2	0.036	-30.885	-30.863	-30.728
2.5	3	0.031	-34.468	-34.448	-34.314
2.6	4	0.021	-38.214	-38.195	-38.062
2.7	5	0.006	-42.119	-42.101	-41.969
2.8	6	-0.012	-46.18	-46.163	-46.0316
2.9	7	-0.032	-50.392	-50.376	-50.245
3.0	9	0.012	-54.763	-54.749	-54.623

E_{SCRPA} . However we should not give this any significance. In order to increase the sensitivity of the results to the accuracy of the theory it is instructive to calculate differences of energies of the ground-state band with L values just one unit away from the absolute ground state. One such quantity is the ‘‘chemical potential’’ which should be identified with the Lagrange multiplier

$$\mu = 1/2(E_{L+1}^0 - E_{L-1}^0). \quad (3.1)$$

In Fig. 2 we show μ where we calculate separately $E_{L\pm 1}^0$ (in RPA and SCRPA) and then take the difference. The calculated values correspond to the crosses and the continuous lines shall guide the eye. We also give in Fig. 2 the L values which correspond for a given x value to the absolute ground state. The same applies to Figs. 3 and 4.

In Fig. 2 we see strong improvement of SCRPA over RPA and the high quality of the results in comparison with the exact values in the region around the phase transition point $x \approx 1$. We also can take the μ values found from adjusting the correct $L = \langle P \rangle$ values in the RPA and SCRPA

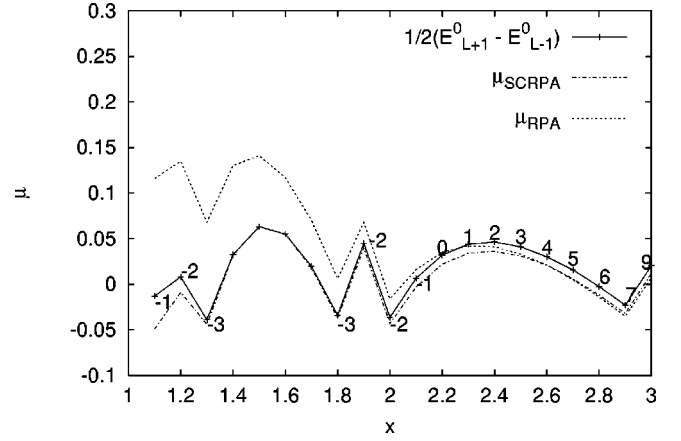


FIG. 2. The difference, Eq. (3.1), between the energies of neighboring states in the ground state band, $E_{L+1}^0 - E_{L-1}^0$, is given for the exact case (full line which connects the calculated values, marked by crosses) for the standard RPA (dotted line), and for SCRPA (dashed dotted line). The numbers on the curve indicate the L value which has the absolute ground state at that x value. Crosses carrying no number are supposed to have the same L value as the last and first L value enclosing the unmarked internal. The calculations are performed for $\alpha = 3$, $N = 30$.

calculations. Within the thickness of the lines these values cannot be distinguished from the previous values, demonstrating the internal consistency of the approach. Two other quantities closely related to the chemical potential are the energy differences of the absolute ground state with its ‘‘left’’ and ‘‘right’’ neighbors just one unit in L away

$$\Delta E_{\pm 1} = E_L^0 - E_{L\pm 1}^0. \quad (3.2)$$

These quantities are interesting because, as we will explain below, they are closely related to the lowest RPA eigenvalue Ω_1 in the symmetry broken phase. We show $\Delta E_{\pm 1}$ in Figs. 3 and 4. Not surprisingly the same very good agreement with the exact results as in the case of μ is found in these cases also. In order to appreciate the quality of the results displayed in the Figs. 2, 3, and 4, we must realize that they

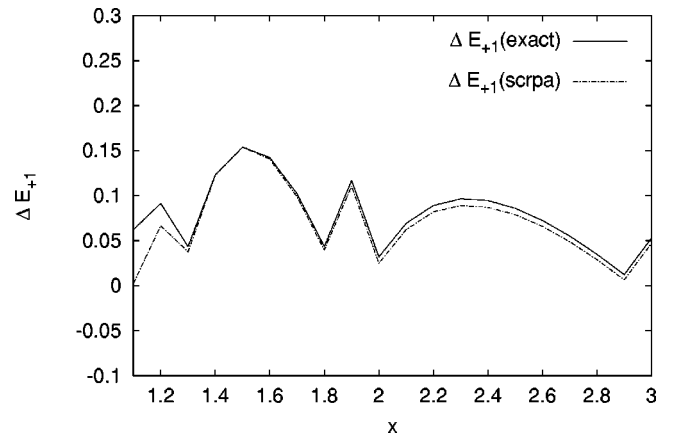


FIG. 3. Comparison between the exact results and the SCRPA results for the excitation energy $|\Delta E_{+1}| = |E_L^0 - E_{L+1}^0|$ in the deformed region. In this graph $\alpha = 3$, $N = 30$.

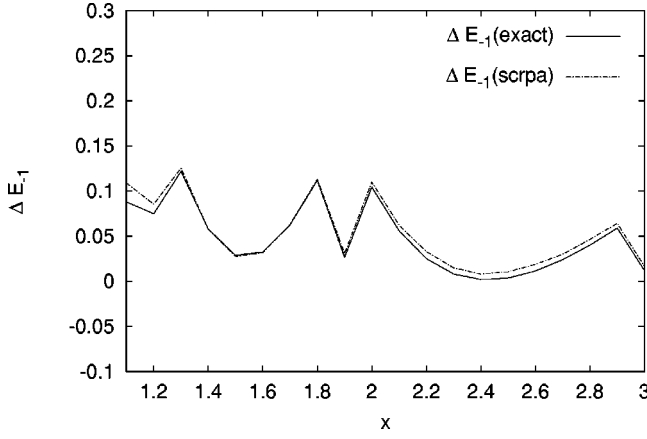


FIG. 4. Comparison between the exact results and the SCRPA results for the excitation energy $|\Delta E_{-1}| = |E_L^0 - E_{L-1}^0|$ in the deformed region. In this graph $\alpha=3$, $N=30$.

represent very small numbers obtained as a difference of two big numbers (ground-state energies). For example for $x=1.2$ the difference between $E_{L-1}^0=2.0367$ and $E_{L+1}^0=-2.0203$ is very small compared to their individual values. We also should notice that the smallness of $\Delta E_{\pm 1}$ means that two neighboring ground states with L and $L \pm 1$, respectively, are almost degenerate which indicates that the system is in the spontaneously broken symmetry phase. One indeed can check that in the large N limit $\Delta E_{\pm 1}$ tends to zero. The zero eigenvalue (the Goldstone mode) which is one of the solutions of the standard RPA in the “deformed” region [7] corresponds to this vanishing of neighboring ground-state energies in the large N limit.

Let us therefore now discuss the eigenvalues of RPA and SCRPA matrices. In Fig. 5 we show the RPA and SCRPA solutions for the highlying eigenvalue Ω_2 .

The 4×4 matrix has eigenvalues $\Omega'_{\pm 1}$, $\Omega'_{\pm 2}$. As we have seen in Sec. II, in standard RPA the lowest eigenvalues correspond in the deformed region to the spurious mode, i.e.,

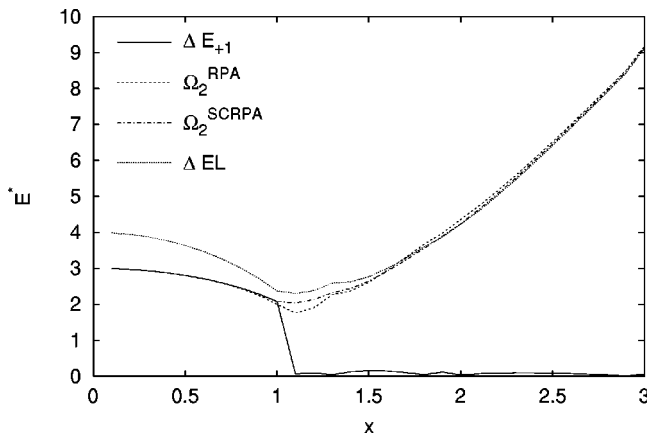


FIG. 5. The RPA and the SCRPA results of the energy of the excitation mode Ω_2 (corrected in both cases) compared with the exact energy of the excitation ΔE_{+1} , $x < 1$, and with the exact energy of the excitation $\Delta E_L = E_L^1 - E_L^0$, $x > 1$. Here $\alpha=3$ and $N=30$.

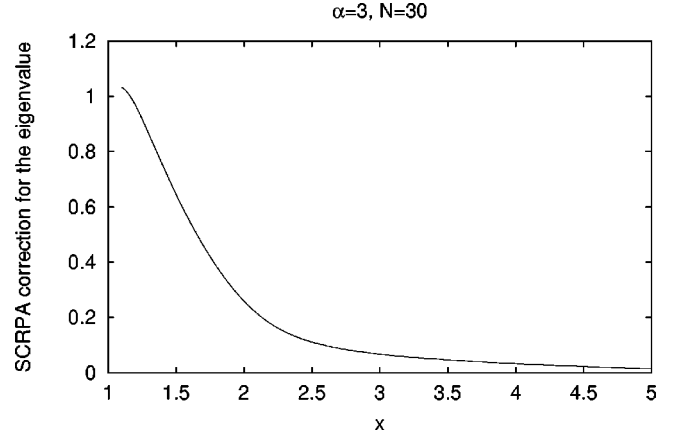


FIG. 6. The difference $[\Omega_2(\text{SCRPA}) - \Omega_2(\text{RPA})]$ as a function of x .

$\Omega'_{\pm 1} = 0$ whereas the second eigenvalue gives the excitation of the intrinsic system. Before coming to the result we should mention again that the RPA eigenvalues in the deformed region are calculated with the “intrinsic” Hamiltonian $H' = H - \mu \hat{P}$. To have the eigenvalues Ω_μ corresponding to H we must correct for the cranking term as already discussed in Sec. II. The results for Ω_2 are presented in Fig. 5. RPA and SCRPA values are compared with exact “intra-band” excitation $\Delta E_{+1} = E_{L+1}^0 - E_L^0$ (low lying state) and the exact interband excitation $\Delta E_L = E_L^1 - E_L^0$ (high lying state).

We first remark the very abrupt phase transition at $x=1$ in the exact case seen for ΔE_{+1} . After the phase transition ΔE_{+1} stays finite but very small decreasing for increasing x and therefore, as usual, for intra-band transitions, ΔE_{+1} corresponds to the Goldstone mode. This we will discuss below. The interband excitation ΔE_L becomes the true “intrinsic excitation” in the deformed region. We therefore see a crossover of Ω_2 from $\Delta E_{+1} = E_{L+1}^0 - E_L^0$ before to ΔE_L after the phase transition. This crossover is the usual scenario when passing from the Wigner-Weyl to the Nambu-Goldstone regime. Unfortunately Ω_2 is again a quantity where there is little distinction between RPA and SCRPA. Nonetheless SCRPA improves significantly over RPA.

In Fig. 6 we display the difference between the eigenvalue Ω_2 calculated with the standard RPA and the one calculated with the SCRPA. This difference, which represents the correction of the SCRPA compared to the RPA standard result, clearly shows the gain in precision SCRPA supplies.

Let us now come to the discussion of the eigenvalue Ω_1 . As we have seen before in standard RPA, this eigenvalue corresponds beyond the phase transition to the Goldstone mode according to the spontaneously broken symmetry, i.e., $\Omega'_1 = 0$. It is standard practice of RPA theory to reestablish the “rotational” excitations in calculating the corresponding inertia via the Thouless-Valatin method [26]. This has been demonstrated in Ref. [16] and we do not want to repeat it here. It is, however, interesting to plot Ω_1 [see Eq. (2.31)] instead of Ω'_1 as we argued we should do in Sec. II to obtain the excitation energies of H and not of H' . This we show in Fig. 7 for standard RPA together with the exact result. For

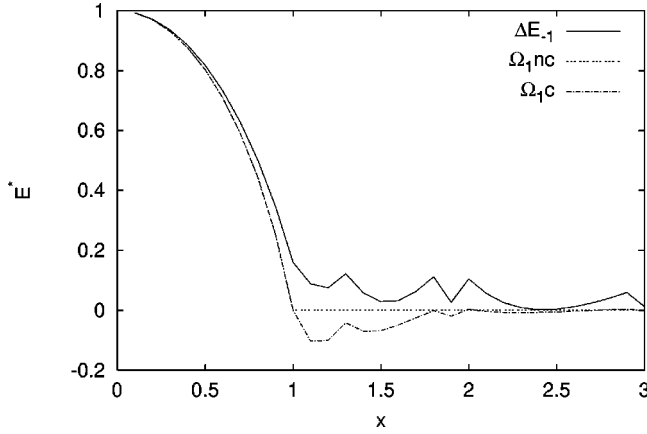


FIG. 7. Comparison, as a function of coupling strength $x = G\sqrt{N}/\alpha$, between exact results for the energy of the first excited state $|\Delta E_{-1}| = |E_L^0 - E_{L-1}^0|$ and the RPA results for the corrected energy of the spurious state Ω_{1C} and the noncorrected energy Ω_{1NC} . In this figure $\alpha = 3$, $N = 30$.

the quantity ΔE_{-1} we see that in spite of giving unphysical results, i.e., “negative excitation energies,” the qualitative behavior is quite similar to the exact result. In fact, as mentioned already, the turning negative of Ω_1 is a consequence of the well-known deficiency of standard RPA that it is overemphasizes correlations for finite systems. Therefore the phase transition point $\Omega_1 = 0$ in Fig. 7 comes too early and the continuation of Ω_1 for $x > 1$ necessarily turns negative. If the behavior $\Omega_1 = \Omega_1(x)$ not only shall stay qualitatively but also quantitatively the same as in the exact solution, one of the hopes of this work was that SCRPA will cure this drawback of RPA. Indeed in another study where pairing correlations in the seniority model were treated via SCRPA this was very nicely the case [27]. Unfortunately in this point our present approach fails for the deformed region. In Fig. 8 we show the SCRPA solution for Ω_1 (together with the exact one and also again RPA) before and after the phase transition point. We see that for $x < 1$ SCRPA nicely corrects the RPA values as expected, but for $x > 1$ the SCRPA results are unphysical.

At first we were quite puzzled by these results because the only difference of the present case with respect to former models is that here fermions and bosons are mixed whereas before we only treated systems of bosons or fermions separately. In fact there is the possibility that our RPA ansatz for the present model with respect to the symmetry operator in the deformed basis [see Eq. (2.14)] is too restricted. We see that P is quadratic in the fermion operators and linear plus quadratic in the Bose operators. Our RPA excitation operators (2.6) contain quadratic terms for fermions but only linear terms for bosons. With respect to the symmetry operator this is clearly an inequivalent treatment. We suspect that if one augments our RPA ansatz by B^+B^+ and BB terms such as

$$Q_\nu^+ = X_{\nu,t^+} - Y_{\nu,t^-} + \lambda_\nu B^+ - \mu_\nu B + U_\nu B^+B^+ - V_\nu BB \quad (3.3)$$

the description of the low-lying mode would be much im-

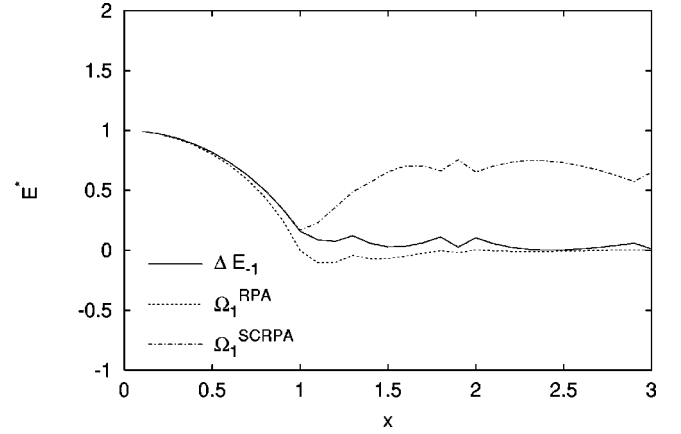


FIG. 8. The RPA and the SCRPA results for the energy of the spurious states Ω_1 (corrected in both cases) compared with the exact energy of the excitation ΔE_{-1} . In this graph $\alpha = 3$, $N = 30$.

proved. Inclusion of these extra terms, however, considerably complicates the theory. Since we were able in this exploratory work to very accurately describe the low lying mode $\Delta E_{\pm 1}$ via the detour of calculating neighboring ground-state energies belonging to the ground-state band separately (see Fig. 1), we feel entitled to present our results without going into these additional complications. This, however, shall be studied in future work.

IV. CONCLUSION

In this work we applied the so-called self-consistent RPA (SCRPA) to a system of interacting fermions and bosons. The case studied is a schematic field theoretical model with usual fermion-boson coupling. The work must be considered as exploratory since before SCRPA has only been applied either to pure fermionic or pure bosonic systems. In this work it is the first time that we treat a fermion-boson mixture. In general we found that SCRPA performs better than standard RPA and in some cases we got rather drastic improvement. However, the model turned out to be slightly unfortunate, since a certain number of quantities are already very well described by standard RPA as, e.g., ground-state energies. The great improvement of SCRPA versus RPA showed up in differences of almost degenerate neighboring states of the ground-state band in the symmetry broken phase belonging to different quantum numbers of the system. These differences tend to zero in the macroscopic limit and are to be considered as the Goldstone modes. We obtained excellent results in calculating neighboring ground-state energies separately and taking the difference. For one quantity we have to signal failure of our present approach. This concerns the low-lying eigenvalue of the SCRPA matrix. This eigenvalue should also represent the same type of Goldstone mode we just discussed. The corresponding SCRPA eigenvalue, is, however, quite far from the exact values. This deficiency is certainly due to our inexperience with coupled fermion-boson systems because for, e.g., a purely fermionic system we could show that the Goldstone mode is reproduced accurately [27]. We suspect that this failure is due to a too restricted ansatz of our RPA operator and we want to

investigate a more general ansatz in the future. The experience gained in this work also can be exploited in future applications of SCRPA to more demanding models such as ϕ^4 Lagrangians as the linear σ model.

In conclusion we found that in this first application of

SCRPA to interacting bosons and fermions the results were generally substantially improved over standard RPA values. However, the Goldstone mode in the symmetry broken phase needs further investigation.

-
- [1] Z. Aouissat, P. Schuck, and J. Wambach, Nucl. Phys. **A618**, 402 (1997).
 - [2] Z. Aouissat, G. Chanfray, P. Schuck, and J. Wambach, Nucl. Phys. **A603**, 458 (1996).
 - [3] J.M. Häuser, W. Cassing, A. Peter, and M.H. Thoma, Z. Phys. A **353**, 301 (1995).
 - [4] A. Kerman and C.Y. Lin, Ann. Phys. (N.Y.) **241**, 185 (1995).
 - [5] P. Ring and P. Schuck, *The Nuclear Many-Body Problem* (Springer-Verlag, Berlin, 1980).
 - [6] J.C. Parikh and D.J. Rowe, Phys. Rev. **175**, 1293 (1968).
 - [7] G. Röpke, M. Schmidt, L. Münchow, and H. Schulz, Nucl. Phys. **A399**, 587 (1983).
 - [8] G. Röpke, Ann. Phys. (Leipzig) **3**, 145 (1994).
 - [9] G. Röpke, Z. Phys. B **99**, 83 (1996).
 - [10] K. Hara, Prog. Theor. Phys. **32**, 88 (1964).
 - [11] D.J. Rowe, Rev. Mod. Phys. **40**, 153 (1968).
 - [12] D.J. Rowe, Phys. Rev. **175**, 1283 (1968).
 - [13] J. Dukelsky and P. Schuck, Phys. Lett. B **464**, 164 (1999).
 - [14] P. Krüger and P. Schuck, Europhys. Lett. **27**, 395 (1994).
 - [15] J. Dukelsky, G. Röpke, and P. Schuck, Nucl. Phys. **A628**, 17 (1998).
 - [16] D. Schütte and J. Da Providencia, Nucl. Phys. **A282**, 518 (1977).
 - [17] B.W. Shore and P.L. Knight, J. Mod. Opt. **40**, 1195 (1993).
 - [18] M. Baranger, Nucl. Phys. **A149**, 225 (1970).
 - [19] M.K. Weigel and J. Winter, J. Phys. G **4**, 1427 (1978).
 - [20] J. Dukelsky and P. Schuck, Mod. Phys. Lett. A **6**, 2429 (1991).
 - [21] J. Dukelsky and P. Schuck, Nucl. Phys. **A512**, 466 (1990).
 - [22] F. Catara, N. Dinh Dang, and M. Sambataro, Nucl. Phys. **A579**, 1 (1994).
 - [23] G. Schalow and M. Yamamura, Nucl. Phys. **A161**, 93 (1971).
 - [24] M. Yamamura, Prog. Theor. Phys. **52**, 538 (1974).
 - [25] S. Nishiyama, Prog. Theor. Phys. **55**, 1146 (1976).
 - [26] D.J. Thouless and J.G. Valatin, Nucl. Phys. **31**, 211 (1962).
 - [27] J. Dukelsky and P. Schuck, Phys. Lett. B **387**, 233 (1996).